

A comment on the colour-colour diagrams of Low Mass X-ray Binaries

Marek Gierliński^{1,2} and Chris Done¹

¹*Department of Physics, University of Durham, South Road, Durham DH1 3LE, UK*

²*Obserwatorium Astronomiczne Uniwersytetu Jagiellońskiego, 30-244 Kraków, Orla 171, Poland*

Submitted to MNRAS

ABSTRACT

Disc accreting neutron stars come in two distinct varieties, atolls and Z sources, named after their differently shaped tracks on a colour-colour diagram as the source luminosity changes. Here we present analysis of three transient atoll sources showing that there is an additional branch in the colour-colour diagram of atoll sources which appears at very low luminosities. This new branch connects to the top of previously known C-shaped (atoll) path, forming a horizontal track where the average source flux decrease from right to left. This turns the C-shape into a Z. Thus both atolls and Z sources share the same topology on the colour-colour diagram, and evolve in similar way as a function of increasing averaged mass accretion rate. This strongly favours models in which the underlying geometry of these sources changes in similar ways. A possible scenario is one where the truncated disc approaches the neutron star when the accretion rate increases, but that in the atolls the disc is truncated by evaporation (similarly to black holes) whereas in the Z sources it is truncated by the magnetic field.

Key words: accretion, accretion discs – X-rays: binaries

1 INTRODUCTION

Low mass X-ray binaries (LMXBs) hosting a neutron star can be observationally divided into two main categories, dubbed atolls and Z sources (Hasinger & van der Klis 1989). This classification is based on changes in both spectral and timing properties as the source varies. Z sources are named after a Z-shaped track they produce on an X-ray colour-colour diagram. Atolls can fall into one of the two spectral states, a hard, low luminosity ‘island’ or a soft, high luminosity ‘banana’. They trace a U-shaped or C-shaped track as the source spectrum evolves between the island and the banana (see e.g. fig. 1 in Méndez et al. 1999). These differences between the two LMXBs categories probably reflect differences in both mass accretion rate, \dot{M} , and magnetic field, B , with the Z sources having high luminosity (typically more than 50 per cent of the Eddington limit) and magnetic field ($B \geq 10^9$ G) while the atolls have lower luminosity (generally less than 10 per cent of Eddington) and low magnetic field ($B \ll 10^9$ G) (Hasinger & van der Klis 1989).

Both atolls and Z sources move *along* their tracks on the colour-colour diagram and do not jump between the track branches. Most of the X-ray spectral and timing properties, e.g. the kilohertz quasi-periodic oscillation (QPO) frequency (Méndez & van der Klis 1999), depend only on the position

of a source in this diagram. This is usually parameterized by the curve length, S , along the track.

This strongly suggests that a single parameter determines the overall properties of the source, generally believed to be the accretion rate, which increases with S from the horizontal (top) to the flaring (bottom) branch in the Z sources, and from the island to the banana in the atolls. The increasing characteristic frequencies in the power spectra along the track are then generally explained by the inner disc radius decreasing as a function of S (e.g. the review by van der Klis 2000). However, the situation is more complex as S is not simply related to the observed X-ray luminosity as would be expected if it is determined by the mass accretion rate (e.g. van der Klis 2000; 2001).

In this letter we present a compilation of *RXTE* data from three transient atoll sources. Their large amplitude of luminosity variation allows us to plot the full track in the colour-colour diagram, which appears to form a shape of ‘Z’, similar to Z sources.

2 THE DATA

We have analysed the *RXTE* observations of the three atoll LMXBs: Aql X-1 (Cui et al. 1998; Reig et al. 2000), 4U 1608–

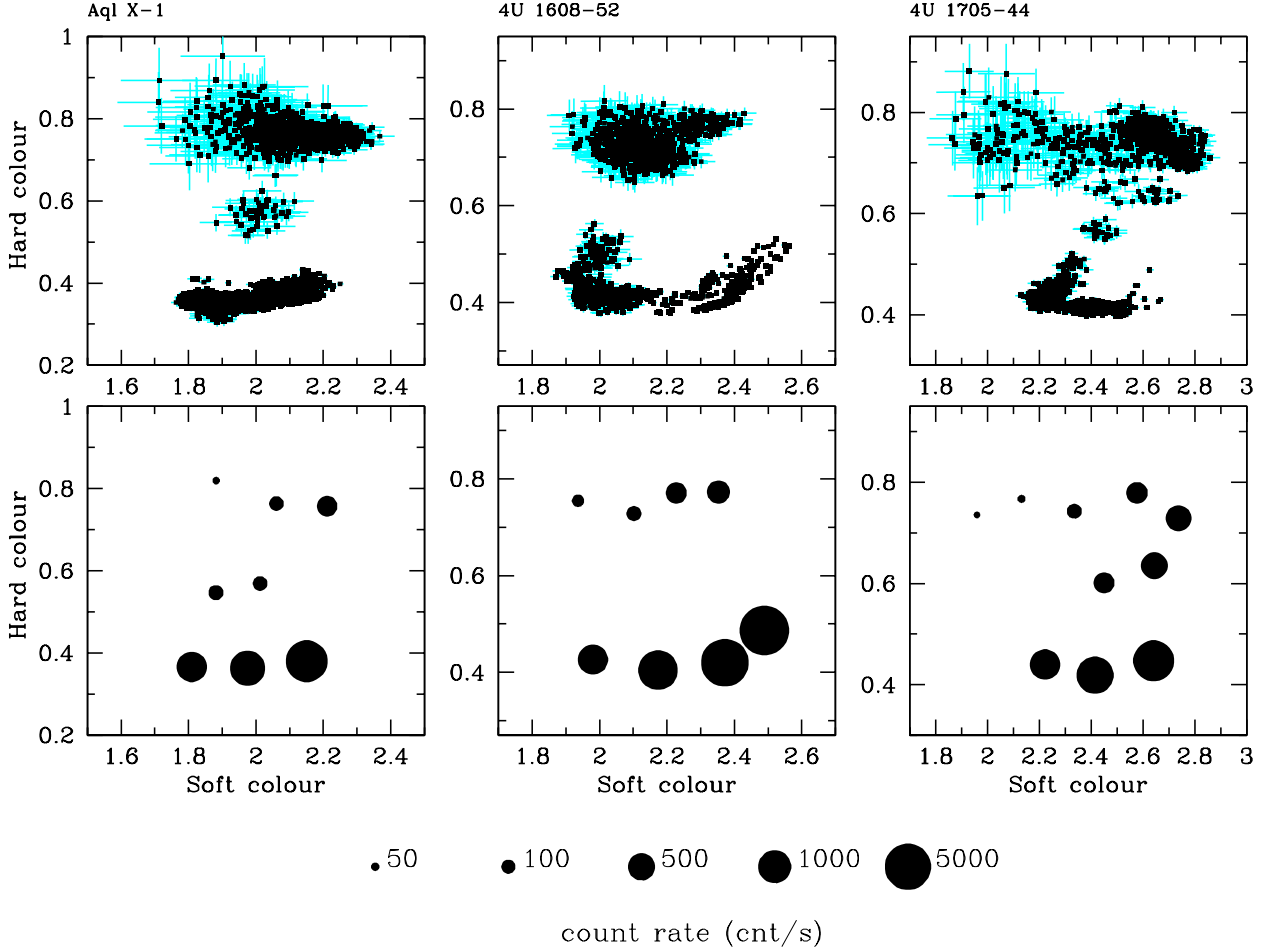


Figure 1. Colour-colour diagrams of three atoll sources. The colours are defined as a ratios of the counts in 4–6.4 keV over 3–4 keV bands (soft) and 9.7–16 over 6.4–9.7 keV bands (hard). The upper panels show original background-subtracted diagrams with the bin size of 128 s. The lower panels contain rebinned data and a size of each data point is proportional to the total count rate in detectors 0, 2 and 3, in the 3–16 keV band.

52 and 4U 1705–44 (Hasinger & van der Klis 1989). 4U 1608–52 is a transient source and its most recent outburst in 1998 was observed by *RXTE* with a good coverage of both island and banana states. Aql X-1 is also a transient, showing outbursts in a time-scale of months to years. 4U 1705–44 is a strongly variable X-ray source, switching between the island and banana states on the time-scales of months.

We have used publicly available *RXTE*/PCA data of these three sources from PCA epochs 3 (between 1996 April 15 and 1999 March 22) and 4 (between 1999 March 22 and 2000 May 13). We selected data from detectors 0, 2 and 3, excluding all type I bursts and observations with very poor statistics. This gave 477 ks of data for Aql X-1, 219 ks for 4U 1608–52 and 172 ks for 4U 1705–44. The PCA light-curves for each energy channel were extracted in 128 s bins. These were used to build a colour-colour diagram, defining a soft colour as a ratio of 4–6.4 to 3–4 keV count rates, and a hard colour as a 9.7–16 over 6.4–9.7 keV ratio.

The response of the PCA detectors is slowly varying as a function of time. Additionally, the high-voltage settings of the instruments were altered between the PCA epochs

3 and 4. Therefore, the energy boundaries of each energy channel change in time, causing a shift in the colours. We have approximately taken these changes into account by reading these boundaries from the response matrices created for the beginning and end of each PCA epoch, and by linearly interpolating between them. When accumulating counts in each of the four energy bands (used for computing the colours), we have interpolated the number of counts for channels on the edges of these energy bands. We have checked the correctness of this procedure using Crab data from various observations in both PCA epochs. We computed colours and noticed that the position of Crab on the diagram still changes in time. This is due to the approximate character of the colours we had calculated. Therefore, to account for this variation, we have calculated multiplicative factors for the colours from the Crab data and applied them to our data (see e.g. Homan et al. 2001 for the similar method). The final result is presented in Fig. 1 (upper panels).

To make these plots clearer and to enhance the evolutionary track on the diagram we have rebinned the data

using a nearest neighbour clustering technique. In each step of the iteration the two nearest bins (data points) on the colour-colour diagram were found. The total numbers of counts in both bins were added and a new count rate and colours were calculated. Thus, the two bins were replaced by one. The procedure was carried on until the assumed number of bins (between 8 and 10, as seen in the lower panels of Fig. 1) was reached. This method gathers together the data with similar spectral properties (colours) as opposed to increasing the length of the time bin, which averages data in time. The result is presented in Fig. 1 (lower panels). The size of the symbol is proportional to the logarithm of the count rate, so it gives an overview of the luminosity changes in the diagram.

3 RESULTS

All three colour-colour diagrams in Fig. 1 show features characteristic of atoll sources that have been known for many years (e.g. van der Klis 1995; Méndez 1999). There is a banana in the lower part and several islands in the upper part of the diagram. The banana is significantly brighter than the islands, and the X-ray flux increases along the banana branch, from left to right.

However, this large compilation of data shows other features which have not previously been seen from sparser data sets. There are *three* distinct branches in the colour-colour diagram. The banana branch forms a lower horizontal track at hard colour of ~ 0.4 , while the island state begins along the diagonal track which connects to the left-hand end of the banana. But there is a part of the diagram not reported before: an upper horizontal branch, at hard colour of ~ 0.7 – 0.8 , connected to the upper right end of the diagonal branch. It is particularly pronounced in 4U 1705–44. This extends the previously known C-shaped pattern into a Z. There were hints of this extension in previous observations of 4U 1705–44 (Langmeier et al. 1989), but this is the first time that it is shown so noticeably.

To show this new branch more clearly we have created a combined colour-colour diagram of all three sources. Since these three atolls have similar spectral and timing properties, they probably have the same underlying accretion geometry and radiation mechanisms. Thus we might expect their spectral evolution, and hence the colour-colour diagrams to be the same, but despite similarities in shape, the colour-colour diagrams of Fig. 1 are *shifted* with respect to each other. This is mainly caused by differences in absorption, which strongly affects the soft colour, but there might also be subtle shifts in hard colour from differences in spin frequency (affecting disc-to-boundary layer luminosity ratio and hence the soft colour as well) and perhaps also the inclination angle. We have attempted to correct for these effects by simply shifting the diagrams in both colours. We have linearly transformed each 128 s data point of each source in a way that the left-hand edge of the lower branch have transformed colours of (1, 1) and the right-hand edge of the upper branch transforms to (2, 2). The resulting diagram of all three sources together is shown in Fig. 2. We can see that the three diagrams coincide very well, and the three branches forming a Z-shaped track are clearly visible.

We have analysed source movement along the Z-shaped

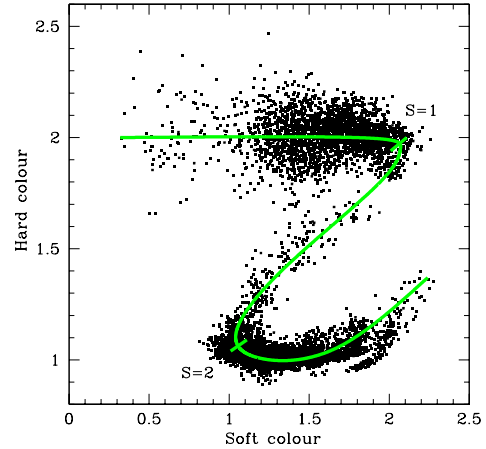


Figure 2. The ‘big picture’ of the atoll sources: a combined colour-colour diagram of Aql X-1, 4U 1608–52 and 4U 1705–44. The colours of the three sources from Fig. 1 were linearly transformed so as to co-align all three systems at turns on the track. The sources clearly define a Z-shaped track. The curve defines the position along the track, S .

track. For this, we have taken the original (i.e. not colour-binned) colour-colour diagram of 4U 1705–44 and traced how the position of the source (in 128 s data bins) moves with time. We confirm that motion in the diagram, including the upper branch, goes *along* the track and we do not notice jumps between the branches (though jumps cannot be completely excluded, since the data is rather sparse in time). 4U 1705–44 can cross the full width of the upper branch in about 10 days, while transition on the diagonal takes about five days (a similar transition in 4U 1608–52 took about three days). The movement in the lower branch is much faster, with time-scales of hours.

The lower panels in Fig. 1 show that the average X-ray flux at a given point on the track increases from left to right (i.e. with increasing soft colour) both in the upper and lower branches. To study the source flux along the track in details, for each grouped point in Fig. 1 we have extracted a typical PCA spectrum from a single *RXTE* pointing (one to three orbits, usually 3–10 ks of exposure) with the same colours and mean count rate. These spectra were fit with a model of a blackbody, Comptonized component and its reflection, with absorption set at 0.5, 1.5 and $1.2 \times 10^{22} \text{ cm}^{-2}$, for Aql X-1, 4U 1608–52 and 4U 1705–44 respectively (Church & Balucińska-Church 2001; Penninx et al. 1989; Predehl & Schmitt 1995). These show that the spectra all along the upper horizontal branch are rather hard, similar to those previously seen in the hardest island states. The bolometric flux was calculated by extrapolating the unabsorbed model spectrum, so it is somewhat model dependent but gives at least a zeroth order correction. In Fig. 3 we plot this bolometric flux in arbitrary units as a function of distance S along the Z track. We have defined the right-hand edge of the upper branch as $S = 1$, and the left-hand edge of the lower branch as $S = 2$ and linearly interpolated to get the S value of all the other data points (see Fig. 2). The bolometric fluxes are scaled so that they are roughly equal at the $S = 1$ point. It is clear that the shapes of these curves

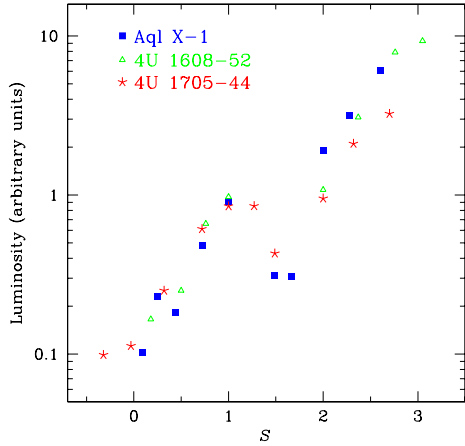


Figure 3. Bolometric luminosity (absorption corrected) as a function of S , i.e. distance along the Z track. The luminosities are linearly scaled so that they match at the $S = 1$ point. The evolution of luminosity as a function of S is remarkably similar for all 3 sources.

are very similar for all 3 sources, showing a steady rise in the upper branch ($S \leq 1$), and then a drop on the diagonal branch, and then rising again along the lower branch.

This *average* bolometric flux most likely corresponds to the average mass accretion rate. Then, extending a LMXB paradigm we suggest that the accretion rate increases along the Z-shaped track in the colour-colour diagram. There is however a *decrease* of the flux on the diagonal branch. We speculate that this might be associated with jet formation. It is known that jets are associated with state transitions in both neutron star and black hole transients (e.g. Fender & Kuulkers 2001). Alternatively, the mass accretion rate onto the central source (and hence the hard X-ray flux) could be reduced if much of the inflowing material was used to extend the disc inwards.

To convert X-ray fluxes into true luminosity requires a distance. For these three sources the best distance estimates are: 3.6 kpc for 4U 1608–52 from radius expansion of X-ray bursts (Nakamura et al. 1989), 4–6.5 kpc for Aql X-1 from optical spectroscopy of the companion star (Rutledge et al. 2001) and 6.3–8.2 kpc for 4U 1705–52 from modelling of X-ray bursts (Haberl & Titarchuk 1994). This gives the $S = 1$ point at 5, 4–10 and 10–17 per cent of Eddington luminosity ($L_{\text{Edd}} = 1.76 \times 10^{38}$ ergs s $^{-1}$), for 4U 1608–52, Aql X-1 and 4U 1705–44, respectively. Since luminosity estimates from X-ray bursts are approximate and might contain unknown systematic errors (see e.g. in ’t Zand et al. 2001), it is possible that the position in the colour-colour diagram of all these three atolls depend on the X-ray luminosity in the same way, and that the $S = 1$ point corresponds to ~ 5 –10 per cent of L_{Edd} .

4 DISCUSSION

The three atolls studied here are transient systems, where the luminosity changes by a factor of $\gtrsim 100$, unlike the majority of atolls which are not very variable. The transients go down to very low luminosities where they show a new track

on the colour-colour diagram which extends the previously known atoll (or C) shaped path into a Z. This new upper branch is clearly distinguished from a simple extension of the previously known C-shaped track. Below $S = 1$, the track turns so that the average source luminosity decreases from right to left on the colour-colour diagram. We propose that all atolls would show such a track if their mass accretion rate could change by a large enough factor, but that their normal, rather small range in variability limits their observed colour-colour diagram to only a small section of the track.

A good example of this is 4U 1728–34, regarded as an archetypal atoll tracing a C-shaped track in the diagram (Méndez & van der Klis 1999; Di Salvo et al. 2001). However, the ratio of the highest to lowest count rate of this source is only about 2.5 (Di Salvo et al. 2001). Therefore, we suggest that the 4U 1728–34 data collected so far shows a colour-colour diagram which is limited to the diagonal and lower branches of a Z track. The source never goes to low enough luminosities to sample much of the upper branch.

Thus, we show that atolls share the same colour-colour topology with the Z sources. With increasing accretion rate they both trace out a similar Z-shaped pattern. Despite this similarity, these two LMXB categories are of course not the same. They differ in the luminosity range required to cover the whole Z track (Z sources are much less variable than the three transient atolls presented here) and in the time taken to trace out the upper and diagonal branches (Z sources move much faster). Another important difference is the luminosity at which the Z-shaped pattern arises. For the Z sources the transition from the upper (horizontal) branch to the diagonal (normal) branch occurs at around 0.5 – $1 L_{\text{Edd}}$, while for the atolls this transition occurs at luminosities about ten times less. There is also a significant difference in the spectral shape in the upper branch: spectra of the atolls are much harder, similar to hard state of black hole candidates.

The differences in luminosity and spectral shape can be reconciled in a model in which the fundamental difference between atolls and Z sources is magnetic field. Evolution along the Z track is caused by the increasing mass accretion rate, \dot{M} , decreasing the inner radius, R_{in} , of a truncated disc. For the atolls the disc is probably truncated by evaporation (e.g. Różańska & Czerny 2000), leading to an inner, optically thin, hot flow which gives the hard X-ray spectrum. However, the evaporation efficiency decreases as a function of increasing mass accretion rate, so this cannot truncate the disc in the Z sources. Instead the truncation is likely to be caused by stronger magnetic field, but here the increased mass accretion rate means that the inner flow is much more optically thick, and so cooler.

We note that after this paper was submitted to MNRAS, another group independently presented very similar results (Muno, Remillard & Chakrabarty, astro-ph/0111370).

ACKNOWLEDGEMENTS

We thank Didier Barret for attracting our attention to the 4U 1705–44 data. We also thank the referee, Michiel van der Klis, and Mariano Méndez for helpful discussions. This

research has been supported in part by the Polish KBN grant 2P03D00514.

REFERENCES

- Church M. J., Bałucińska-Church M., 2001, *A&A*, 369, 915
- Cui W., Barret D., Zhang S. N., Chen W., Boirin L., Swank J., 1998, *ApJ*, 502, L49
- Di Salvo T., Méndez M., van der Klis M., Ford E., Robba N. R., 2001, *ApJ*, 546, 1107
- Fender R. P., Kuulkers E., 2001, *MNRAS*, 324, 923
- Ford E. C., van der Klis M., Kaaret P., 1998, *ApJ*, 498, L41
- Ford E. C., van der Klis M., Méndez M., van Paradijs J., Kaaret P., 1999, *ApJ*, 512, L31
- Fortner B., Lamb F. K., Miller G. S., 1989, *Nature*, 342, 775
- Haberl F., Titarchuk L., 1994, *A&A*, 299, 414
- Hasinger G., van der Klis M., 1989, *A&A*, 225, 79
- Homan J., van der Klis M., Jonker P. G., Wijnands R., Kuulkers E., Méndez M., Lewin W. H. G., 2001, astro-ph/0104323
- Lamb F. K., 1989, in Proc. 23 ESLAB Symp. on X-Ray Astronomy, ed. N. E. White, ESA SP-296 (Noordwijk: ESA)
- in 't Zand J. J. M., et al., 2001, astro-ph/0104285
- Langmeier A., Sztajno M., Hasinger G., Trümper J., Gottwald M., 1987, *ApJ*, 323, 288
- Méndez M., 1999, in Proceedings of the 19th Texas Symposium in Paris, published in electronic form
- Méndez M., van der Klis M., 1999, *ApJ*, 517, L51
- Méndez M., van der Klis M., Ford E. C., Wijnands R., van Paradijs J., 1999, *ApJ*, 511, L49
- Nakamura N., Dotani T., Inoue H., Mitsuda K., Tanaka Y., Matsuoka M., 1989, *PASJ*, 41, 617
- Nowak M. A., 2000, *MNRAS*, 318, 361
- Penninx W., Damen E., Tan J., Lewin W. H. G., van Paradijs J., 1989, *A&A*, 208, 146
- Predehl P., Schmitt J. H. M. M., 1995, *A&A*, 293, 889
- Psaltis D., Norman C., 2000, astro-ph/0001391
- Reig P., Méndez M., van der Klis M., Ford E. C., 2000, *ApJ*, 530, 916
- Rózańska A., Czerny B., 2000, *MNRAS*, 316, 473
- Rutledge R. E., Bildsten L., Brown E. F., Pavlov G. G., Zavlin V. E., 2001, *ApJ*, 559, 1054
- van der Klis M., 1995, in Lewin W. H. G., van Paradijs J., van den Heuvel E. P. J., eds., *X-ray Binaries*, Cambridge University Press, Cambridge, P. 252
- van der Klis M., 2000, *ARAA*, 38, 717
- van der Klis M., 2001, *ApJ*, 561, 943
- Wijnands R., van der Klis M., 1999, *ApJ*, 514, 939